Abnormal Curves in a Zermelo Navigation Problem in the Plane and the Fan Shape of Small Time Balls

Bernard Bonnard, Olivier Cots, Joseph Gergaud, Boris Wembe

Abnormal Curves in a Zermelo Navigation Problem in the Plane and the Fan Shape of Small Time Balls

B. Bonnard[*], O. Cots[†], J. Gergaud[‡], B Wembe[§]

July 24, 2020

Abstract

In this note, motivated by the Zermelo navigation problem in the flat plane, where the current field is associated to a point vortex, we discuss the role of the abnormal curves in the shape of the small time balls. Abnormal curves are occurring in the strong current domain in the vicinity of the vortex and form with the hyperbolic geodesics the boundaries of the small time accessibility sets and give to the small time balls a fan shape. Implications with the regularity of the value function are discussed.

Keywords: Helhmoltz-Kirchhoff N vortices model, Zermelo navigation problem, Geometric optimal control, Abnormal curves, Time minimal value function.

1 Introduction

Consider the Zermelo navigation problem in the plane, with a vortex singularity introduced in [5] and whose dynamics is given in cartesian coordinates $q := (x, y) \in M := \mathbb{R}^2 \setminus \{0\}$ by

$$\dot{q}(t) = F_0(q(t)) + u_1(t)\, F_1(q(t)) + u_2(t)\, F_2(q(t)) \tag{1}$$

where F_0 is the current (or drift), and F_1, F_2 define the control directions associated to the heading angle α of the ship:

$$F_0(q) := \frac{\mu}{x^2+y^2}\left(-y\frac{\partial}{\partial x} + x\frac{\partial}{\partial y}\right), \quad F_1(q) := \frac{\partial}{\partial x}, \quad F_2(q) := \frac{\partial}{\partial y}, \qquad \mu > 0,$$

and where $u := (u_1, u_2)$ is the control. The control is bounded by

$$\|u\| := \sqrt{u_1^2 + u_2^2} \leq 1$$

and for $\|u\| = 1$, it is related to the heading angle α by $u = (\cos\alpha, \sin\alpha)$.

Following the control point of view [6], the Zermelo navigation problem is restated as a time minimal control problem to steer q_0 to q_1 for any pair q_0, $q_1 \in M$. We refer to [2] for the differential geometric frame in the case of a weak current and Randers metrics. More generally, our study will concern the local problem and we can consider the general case in an open subset Ω of $\mathbb{R}^2$ where F_0 is smooth, and the control directions are associated to $\|u\| \leq 1$ and where F_1, F_2 form an orthonormal frame for a Riemannian metric g so that $\|u\| = 1$ is the standard unit sphere. In this general frame, for $q_0 \in \Omega$ we can encountered three cases:

- **Weak current case** if $\|F_0(q_0)\|_g < 1$;
- **Strong current case** if $\|F_0(q_0)\|_g > 1$;
- **Intermediate current case** in the transitional case $\|F_0(q_0)\|_g = 1$.

[*]Institut de Mathématiques de Bourgogne, Dijon, France, bbonnard@u-bourgogne.fr
[†]ENSEEIHT, IRIT, Toulouse, France, olivier.cots@irit.fr
[‡]ENSEEIHT, IRIT, Toulouse, France, joseph.gergaud@irit.fr
[§]Université Paul Sabatier, IRIT, Toulouse, France, boris.wembe@irit.fr

The set of admissible controls $\mathcal{U}$ is the set of measurable mappings u from $[0,+\infty)$ to the unit closed Euclidian ball. For $u \in \mathcal{U}$ we denote by $q(\cdot, q_0, u)$ the trajectory of (1) associated to u, initiating at time 0 from q_0 and defined on a domain $[0, t_f(u)]$. The *accessibility set* from q_0 in time $t_f \geq 0$ is denoted by

$$\mathcal{A}(q_0, t_f) \coloneqq \{q(t_f, q_0, u) \mid u \in \mathcal{U} \text{ and } q(\cdot, q_0, u) \text{ is defined on } [0, t_f]\}$$

and the *accessibility set* from q_0 is $\mathcal{A}(q_0) \coloneqq \bigcup_{t_f \geq 0} \mathcal{A}(q_0, t_f)$. In the case of system (1) associated to the vortex problem, from [5], for each pair (q_0, q_1) in the punctured plane there exists a time minimal solution to steer q_0 to q_1. Fixing q_0 we define the *time minimal value function*

$$T(q_0, q_1) \coloneqq \inf_{u \in \mathcal{U}} t_f \quad \text{s.t} \quad q(t_f, q_0, u) = q_1.$$

Fixing q_0, the *sphere* $\mathrm{S}(q_0, r)$ with radius r is the set of points q_1 which can be reached from q_0 in minimum time r, while the *ball* with radius r is $\mathrm{B}(q_0, r) \coloneqq \bigcup_{r' \leq r} \mathrm{S}(q_0, r')$.

The objective of this note is to complete the results of [5] to describe the balls with a small radius. In the weak current case, the result is well known but in the strong current case, the small time accessibility set is bounded by the so-called abnormal curves and the ball has the shape of a *fan*. Our study is based on [4] which describes the shape of the accessibility set in a neighborhood of a reference trajectory under generic assumption. Following the Caratheodory-Zermelo-Goh point of view, our system is extended in the 3D-space, where the control is taken as the derivative $\dot{\alpha}$ of the heading angle and the accessibility set is described in a *conic neighborhood* of the heading angle of the reference curve. Also, in this approach, our analysis relies to consider both time minimizing and maximizing trajectories.

Combined with integrability results of the geodesic flow, due to the rotational symmetry in the vortex problem, it will allow in a forthcoming article to classify the shape of the balls for *general radii* and to classify the *singularities of the value function*.

2 Pontryagin maximum principle and geodesics classification

According to the Maximum Principle [9] and thanks to [5] every minimizing curves is a solution of the C^∞ Hamiltonian dynamics on T^*M given in canonical coordinates $z = (q, p)$ by

$$\dot{z}(t) = \overrightarrow{H}(z(t)) \tag{2}$$

where p is the nonzero adjoint, where

$$\overrightarrow{H} \coloneqq \frac{\partial H}{\partial p}\frac{\partial}{\partial q} - \frac{\partial H}{\partial q}\frac{\partial}{\partial p}$$

is the symplectic gradient associated to the *true* (or maximized) Hamiltonian H given by

$$H(z) \coloneqq H_0(z) + \sqrt{H_1^2(z) + H_2^2(z)},$$

where $H_i(z) \coloneqq p \cdot F_i(q)$ is the Hamiltonian lift of F_i and where $\cdot$ denotes the scalar product. An *extremal* is a solution $t \mapsto z(t)$ of $\overrightarrow{H}$ and the q-projection is called a *geodesic*. Note that $H =: -p^0$ is constant along any extremal and an extremal is called *hyperbolic* if $p^0 < 0$, elliptic if $p^0 > 0$ and abnormal (or exceptional) if $p^0 = 0$. Moreover, thanks to the Maximum Principle, hyperbolic (resp. elliptic) extremals are candidates to the time minimal (resp. maximal) problem, while the time optimality status of the abnormal extremals have been clarified in [4].

A brief recap adapted to the 2-dimensional Zermelo navigation problem is presented here. The first step, using the Zermelo-Caratheodory-Goh point of view, is to parameterize the extremal controls by the derivative of the heading angle α instead of α and this means to extend our system into the single-input (affine) system:

$$\dot{\tilde{q}} = X(\tilde{q}) + v\,Y(\tilde{q}) \tag{3}$$

with $\tilde{q} \coloneqq (q, \alpha)$, $X(\tilde{q}) \coloneqq F_0(q) + (\cos\alpha\, F_1(q) + \sin\alpha\, F_2(q))$ and $Y(\tilde{q}) \coloneqq \frac{\partial}{\partial\alpha}$. In this prolongation, extremal curves $z = (q, p)$ extend into *singular extremal curves* $\tilde{z} \coloneqq (q, \alpha, p, p_\alpha)$ of (3) for the extended Hamiltonian

$$\tilde{H} = \tilde{p} \cdot (X(\tilde{q}) + v\,Y(\tilde{q}))$$

with the constraint $p \cdot Y(\tilde{q}) = 0$.

We assume the following:

Assumptions 2.1 *Take a reference extremal $t \mapsto z(t)$ on $[0, t_f]$, $z = (q, p)$ and let $\tilde{z} = (\tilde{q}, \tilde{p})$ be its extension. Besides, we assume the following: Along γ,*

(A1) *X, Y are linearly independent;*

(A2) *Y, $[X, Y]$ are linearly independent;*

(A3) $[Y, [X, Y]] \notin \mathrm{Span}\{Y, [X, Y]\}$.

From (A3), p is unique up to a factor and the geodesic is strict and moreover singular control v can be computed as a true feedback:

$$v = -\frac{D'(\tilde{q})}{D(\tilde{q})},$$

where we denote:

$$D \coloneqq \det(Y, [Y, X], [[Y, X], Y]),$$
$$D' \coloneqq \det(Y, [Y, X], [[Y, X], X]).$$

Moreover, if we introduce $D'' \coloneqq \det(Y, [Y, X], X)$ we have:

Definition 2.1 *Under assumptions (A1), (A2) and (A3), a geodesic is called:*

- hyperbolic *if* $DD'' > 0$,
- elliptic *if* $DD'' < 0$,
- abnormal *(or* exceptional*) if* $D'' = 0$.

They have the following interpretation: define the extremity mapping at time t_f by $E^{t_f} : v \mapsto \tilde{q}(t_f, \tilde{q}_0, v)$ (t_f, $\tilde{q}_0$ being fixed) and the extremity mapping $E \colon v \to \tilde{q}(\cdot, \tilde{q}_0, v)$ (only $\tilde{q}_0$ being fixed), one has the following.

Proposition 2.2 *Hyperbolic and elliptic extremals correspond to singularities of the extremity mapping (for the L^∞-norm on the set of inputs) for fixed t_f, while abnormal (or exceptional) extremals correspond to singularities of the extremity mapping.*

Moreover, a precise description of the accessibility set in time t_f can be obtained in a C^0-neighborhood of a reference singular extremal under generic assumptions that we described briefly. Dealing with the time minimal control problem, one can assume that $t \mapsto z(t)$ is a one-to-one immersion so that the extension can be identified to $\gamma \colon t \mapsto (t, 0, 0)$ and the singular control v can be taken as $v \equiv 0$, using a proper feedback.

Then, one has:

Proposition 2.3 *In the hyperbolic (resp. elliptic) case, the reference trajectory γ is time minimizing (resp. maximizing) with respect to all trajectories contained in a tubular neighborhood if the final time t_f is less than the first conjugate time t_{1c}. A conjugate time corresponding to a singularity of the exponential mapping $\exp_{q_0} : (t, p_0) \mapsto \Pi(\exp t\vec{H}(q_0, p_0))$ with $\Pi(q, p) \coloneqq q$. In the exceptional case, the reference extremal is time minimizing and time maximizing.*

Moreover one has a precise description of the accessibility set in the tubular neighborhood given by Figure 1. In particular for $t > t_{1c}$, the fixed time extremity mapping becomes open.

In the abnormal case, the abnormal reference trajectory corresponds to a singularity of the extremity mapping and the projection in the singular direction (note that the singular direction depends on the case) is given by Figure 2.

Note due to the small dimension, conjugate points cannot occur and the extremity mapping is never open. In higher dimension, conjugate points can occur either if the fixed time extremity mapping becomes open or in the *generic case* if the extremity mapping becomes open, see Figure 3.

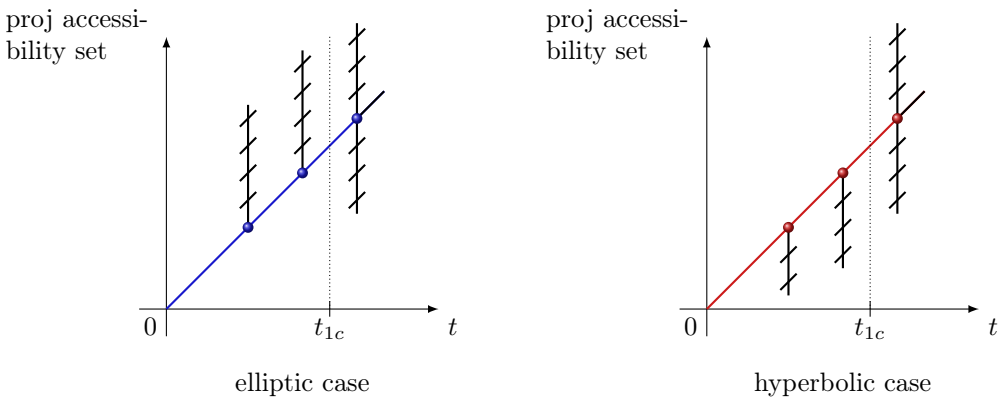

Figure 1: Projection of the fixed time accessibility set in the singular direction.

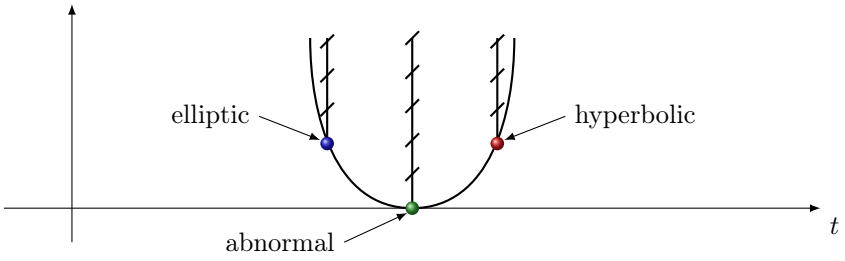

Figure 2: Projection of the accessibility set in the singular direction.

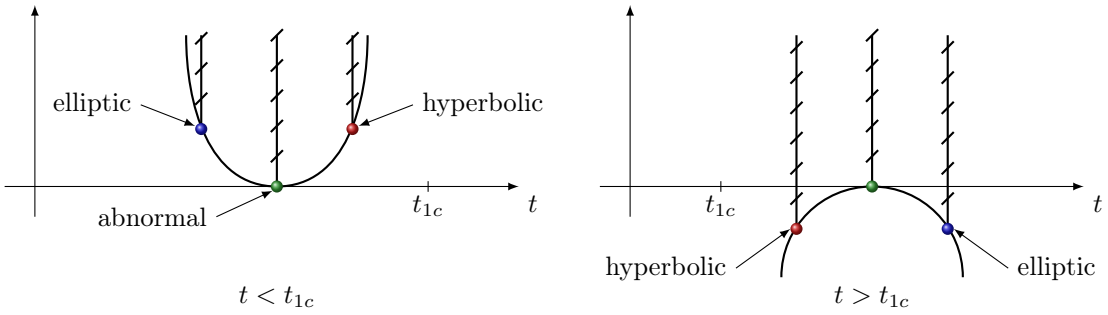

Figure 3: Case $n > 3$: generic conjugate point t_{1c} in the abnormal case.

3 Spheres with small radius

3.1 Notations and definitions

The geodesics are parameterized by t and the initial heading angle α. Fixing q_0 and $t > 0$ we denote by $\exp_{q_0,t}$ the *exponential mapping* $\exp_{q_0,t}\colon \alpha \mapsto \Pi(\exp t\vec{H}(q_0, p_0(\alpha)))$ where $\Pi(q,p) = q$ is the q-projection. A *conjugate point* along a reference geodesic is a point where the exponential mapping is not an immersion and taking the set of first conjugate points they will form the *conjugate locus* $C(q_0)$. A *cut point* is the first point where the geodesic loses optimality and they will form the *cut locus* $\Sigma(q_0)$. The *separating set* $L(q_0)$ is the set of points where two minimizing geodesics starting from q_0 are intersecting.

3.2 Ball and sphere of directions

One consider the smooth Zermelo navigation problem. One can assume that g is the Euclidian metric and F_0 is vertical at the initial point q_0 which can be identified to $q_0 = 0$. The *ball of directions* at q_0 is defined by the set

$$F(q_0) \coloneqq \{F_0(q_0) + u \mid \|u\| \leq 1\}, \tag{4}$$

whose boundary is a circle in our context. We have three cases:

Case 1: Strong current case (Figure 4). In this case the cone of directions is a translation of the unit sphere and we have two *abnormal directions* defined by $\{-\alpha_1, \alpha_1\}$ corresponding to the tangents to the circle from the initial point identified to 0. The *upper part* corresponds to the *hyperbolic directions* and the *lower part* to the *elliptic directions*.

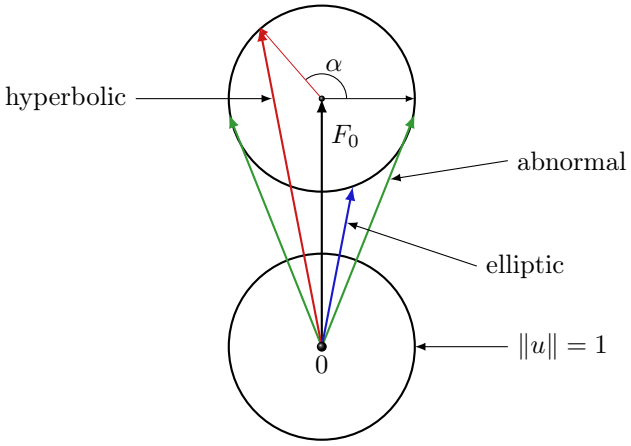

Figure 4: Strong current case.

Cases 2-3: Weak and intermediate current cases (Figure 5). In the intermediate current case the abnormal directions degenerate into the single point 0 and we have only an hyperbolic sector. In the weak drift case, we have only hyperbolic directions.

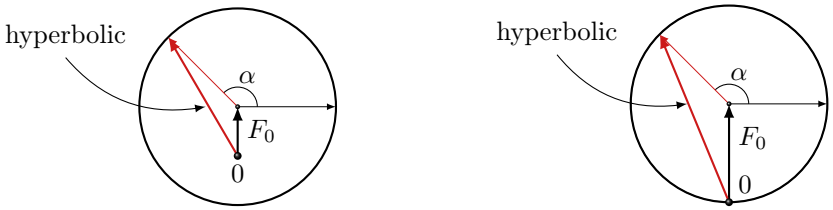

Figure 5: Weak (left subgraph) and intermediate (right subgraph) current cases.

3.3 Small balls and spheres

For small times, the ball of directions $F(q_0)$ gives the shape of the small balls and spheres and it is in accordance with the results of Section 2 about the properties of the extremity mapping.

First case: weak current drift. It corresponds to a Randers problem in the plane, in the frame of the Finsler geometry, see [1].

Proposition 3.1 *In the weak current case, the exponential mapping for small time t is a diffeomorphism from the unit circle to the sphere with radius r and it is represented on Figure 6.*

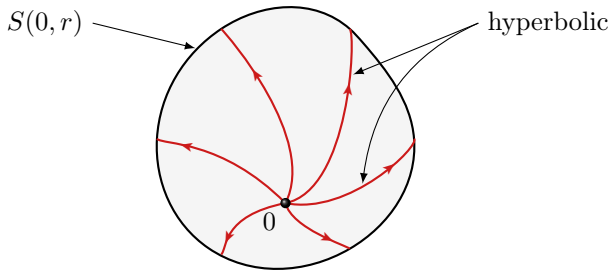

Figure 6: Small sphere and ball for Randers metrics.

Second case: strong drift case. In this case, according to the cone of directions, the small balls have a *fan shape* represented on Figure 7.

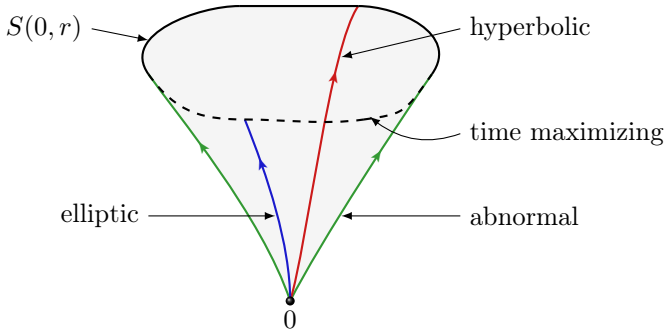

Figure 7: Small sphere and ball for the strong current case.

Proposition 3.2 *In the strong current case, the exponential mapping for a small time is a diffeomorphism from the unit circle onto its image, which is formed on the the upper part by the extremities of the hyperbolic trajectories, the lower part being the extremities of the elliptic trajectories, the two parts being separated by the two points corresponding to the abnormal trajectories. Hyperbolic and abnormal points correspond to the time minimizing trajectories, while elliptic points correspond to time maximizing trajectories. sector.*

Remark 3.3 *This result is in accordance with the geometric analysis of the accessibility set in time t near the reference extremal and corresponds to the three cases presented on Figure 8.*

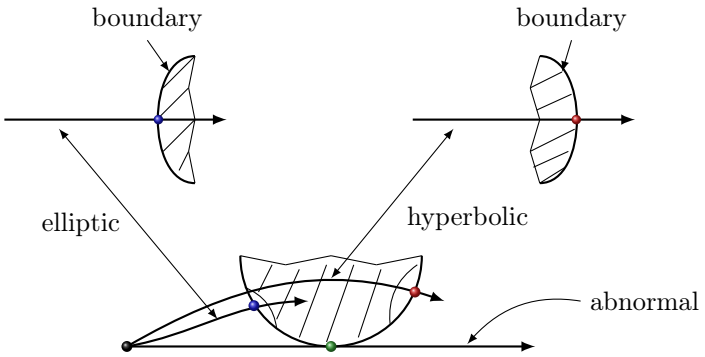

Figure 8: Boundary of the small time accessibility set in time t.

4 The historical Caratheodory-Zermelo model

The main features of the weak current case were already given in the historical work which describes the global minimizing solutions. The objectives of this section is to provide the geometric optimal control frame, see [6].

4.1 The case of revolution

One can consider a general Zermelo navigation problem with a rotational symmetry described in normal coordinates by the pair:

$$F_0(q) \coloneqq \mu(y)\frac{\partial}{\partial x}, \quad g \coloneqq m^2(y)dx^2 + dy^2$$

where μ and $m > 0$ are smooth functions. Hence the system

$$\dot{\tilde{q}} = X(\tilde{q}) + v\,Y(\tilde{q})$$

gives the following:

$$X(\tilde{q}) = (\mu(y) + \cos(\alpha))\frac{\partial}{\partial x} + \frac{\sin(\alpha)}{m(y)}\frac{\partial}{\partial y} \quad \text{and} \quad Y(\tilde{q}) = \frac{\partial}{\partial \alpha}.$$

Straighforward computations lead to:

$$\begin{aligned}
[Y, X](\tilde{q}) &= -\frac{\cos\alpha}{m(y)}\frac{\partial}{\partial x} + \sin\alpha\frac{\partial}{\partial y},\\
[[Y, X], Y](\tilde{q}) &= \frac{\sin\alpha}{m(y)}\frac{\partial}{\partial x} + \cos\alpha\frac{\partial}{\partial y},\\
[[Y, X], X](\tilde{q}) &= \frac{m'(y)}{m^2(y)}(1 + \mu(y)\cos\alpha)\frac{\partial}{\partial x} + \mu'(y)\cos\alpha\frac{\partial}{\partial y}.
\end{aligned}$$

and

$$D(\tilde{q}) = -\frac{1}{m(y)}, \quad D'(\tilde{q}) = -\frac{\cos\alpha}{m(y)}\mu'(y) - \frac{m'(y)}{m(y)}(1 + \mu(y)\cos\alpha)\sin\alpha, \quad D''(\tilde{q}) = -\frac{m'(y)}{m(y)}(1 + \mu(y)\cos\alpha).$$

Hence, the dynamics is given by:

$$\begin{aligned}
\dot{x} &= \mu(y) + \cos\alpha,\\
\dot{y} &= \frac{1}{m(y)}\sin\alpha,\\
\dot{\alpha} &= -\mu'(y)\cos^2\alpha - \frac{m'(y)}{m(y)}\,(1 + \mu(y)\cos\alpha)\sin\alpha.
\end{aligned} \tag{5}$$

Moreover, the condition

$$\frac{\partial H}{\partial \alpha} = 0,$$

where H is the non-maximized Hamiltonian $H = H_0 + H_1\cos\alpha + H_2\sin\alpha$, gives the Clairaut relation:

$$p_x = \frac{m(y)}{\tan\alpha}p_y = cst.$$

Since $H = -p^0$ is constant one gets

$$\mu(y) + p^0\frac{m(y)}{p_x\tan\alpha} = -2\cos\alpha.$$

Hence, we deduce the following:

Proposition 4.1 *In the case of revolution, the dynamics* (5) *can be integrated by quadratures.*

4.2 Historical example

Using the previous section, one can get the geodesics parameterization of the Caratheodory-Zermelo case. One has:

$$X(\tilde{q}) = \sin(\alpha)\frac{\partial}{\partial x} + (y + \cos(\alpha))\frac{\partial}{\partial y} \quad \text{and} \quad Y(\tilde{q}) = \frac{\partial}{\partial \alpha}.$$

The dynamics reduces to:

$$\dot{x} = y + \cos\alpha, \quad \dot{y} = \sin\alpha, \quad \dot{\alpha} = -\cos^2\alpha. \tag{6}$$

We obtain:

Proposition 4.2 *For a given initial point $q_0 = (x_0, y_0, \alpha_0)$, the solution $q(t, q_0) = (x(t, q_0), y(t, q_0), \alpha(t, q_0))$ of the previous system is given by:*

$$\begin{aligned}
&\alpha(t, q_0) = -\arctan(t + c), \quad \textit{with} \quad c = -\tan\alpha_0,\\
&y(t, q_0) = -\frac{p^0}{p_x} - \frac{1}{\cos\alpha(t)},\\
&x(t, q_0) = \frac{1}{2}\ln\left(\frac{\cos\alpha(t)}{1+\sin\alpha(t)}\right) + \frac{\tan\alpha(t)}{2\cos\alpha(t)} - \frac{p^0}{p_x}t - \frac{1}{2}\ln\left(\frac{\cos\alpha_0}{1+\sin\alpha_0}\right) + \frac{\tan\alpha_0}{2\cos\alpha_0} + x_0.
\end{aligned}$$

Proof 1

$$\dot{\alpha} = -\cos^2\alpha \Rightarrow \frac{\dot{\alpha}}{\cos^2\alpha} = -1 \Rightarrow \tan\alpha(t) = -(t + c) \Rightarrow \alpha(t) = -\arctan(t + c), \quad \textit{with} \quad c = -\tan\alpha_0.$$

On the other hand,

$$\begin{aligned}
H = -p^0 \quad &\Rightarrow \quad y p_x + \sqrt{p_x^2 + p_y^2} = -p^0\\
&\Rightarrow \quad p_x y(t) = -p^0 - |p_x|\sqrt{1 + \tan^2\alpha(t)}\\
&\Rightarrow \quad y(t) = -\frac{p^0}{p_x} - \frac{1}{\cos\alpha(t)},
\end{aligned} \tag{7}$$

re-injecting y in $\dot{x} = y + \cos\alpha$ gives us

$$\dot{x}(t) = -\frac{p^0}{p_x} - \frac{1}{\cos\alpha(t)} + \cos\alpha(t)$$

and integrating this equation leads to

$$x(t) = \frac{1}{2}\ln\left(\frac{\cos\alpha(t)}{1+\sin\alpha(t)}\right) + \frac{\tan\alpha(t)}{2\cos\alpha(t)} - \frac{p^0}{p_x}t - \frac{1}{2}\ln\left(\frac{\cos\alpha_0}{1+\sin\alpha_0}\right) + \frac{\tan\alpha_0}{2\cos\alpha_0} + x_0.$$

Abnormals and cusp point: In the abnormal case one has $p^0 = 0$, then:

$$H = -p^0 \;\Rightarrow\; y\,p_x = -\|p\| \;\Rightarrow\; y_0\,p_x = -1 \;\Rightarrow\; p_x = -\frac{1}{y_0},$$

i.e

$$\alpha_a^1 = \arccos\left(-\frac{1}{y_0}\right), \qquad \alpha_a^2 = -\arccos\left(-\frac{1}{y_0}\right).$$

We have a cusp point if and only if $\dot{x}(t_{\text{cusp}}) = \dot{y}(t_{\text{cusp}}) = 0$ i.e $p_{y_{\text{cusp}}} = 0$ and $y_{\text{cusp}} = \pm 1$. Hence, $y_{\text{cusp}} = 1$ if $y_0 > 0$ and $y_{\text{cusp}} = -1$ if $y_0 < 0$.

As illustrated in the figure 10, the cusp point along an abnormal is the limit of a sequence of self-intersections along hyperbolic curves contained in a neighborhood of this abnormal.

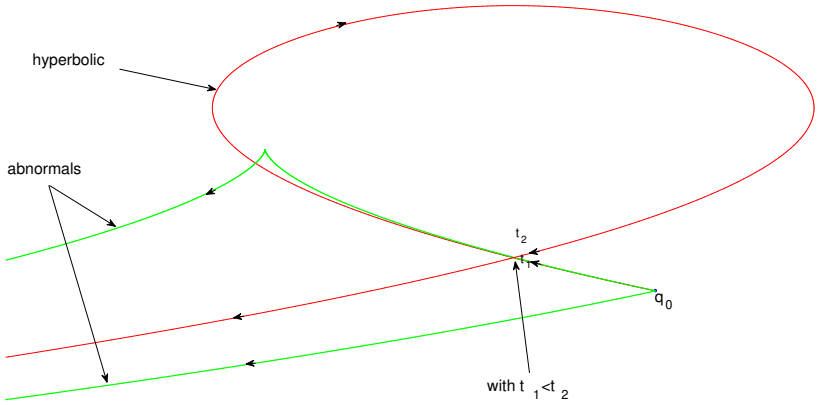

Figure 9: Illustration of the flow of geodesics. On this figure one can see an hyperbolic curve which loses its optimality when intersecting the abnormal for the second time (this highlights the non-continuity of the value function along this abnormal up to the cusp point).

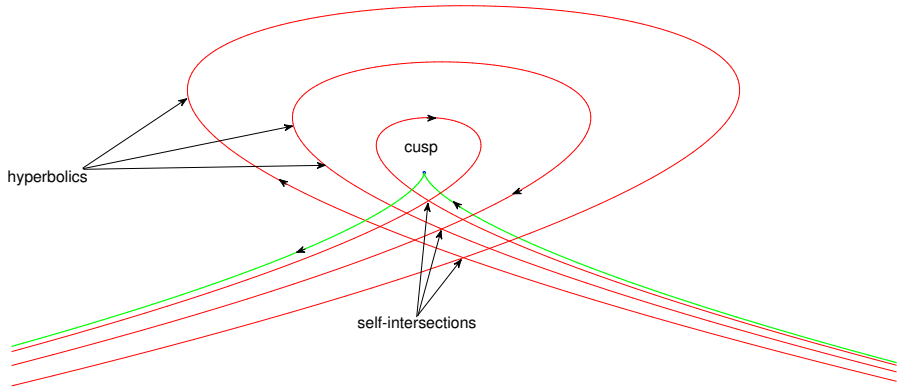

Figure 10: This figure highlights the cusp point along the abnormal which can be seen as the limit of self-intersections that occur along hyperbolic geodesics in a neighbourhood (in the sense of the initial alpha angle) of this abnormal.

5 Conclusion

In this short paper, Zermelo navigation problem in the plane has been set in the frame of geometric optimal control. The sphere of small radius have been described in the case of weak current, this corresponds to the Finsler case, similar to the Riemannian case. If the current is strong, the small ball has a fan shape with two limit directions corresponding to the abnormal geodesics.

The historical Caratheodory-Zermelo [7] is analyzed in this frame. Thanks to the integrability properties of the geodesics flow the problem can be analyzed in full details. One can observe two interesting new phenomena which correspond to stable situations. First of all, when meeting the collinearity set, the abnormal direction

presents a cusp singularity and normal geodesics in a micro-local sector have self-intersections. Second, due to the existence of the abnormal geodesics, the value function is not in general continuous.

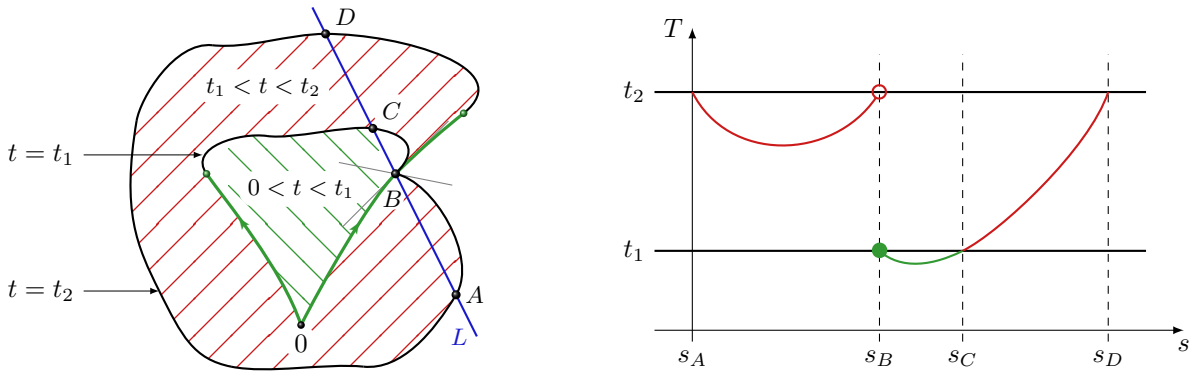

Figure 11: Discontinuity of the time minimal value function T. Let consider two times $0 < t_1 < t_2$, with t_1 small and t_2 large enough. (Left) Balls of radii t_1 and t_2 with the corresponding spheres. The value function T is discontinuous at B, at the intersection of the right abnormal of length t_1 and a hyperbolic extremal of length t_2. (Right) The time minimal value function T along the line L parameterized by s and such that the coordinates value s_A, s_B, s_C and s_D correspond respectively to the points A, B, C and D. One can see the discontinuity of T at s_B.

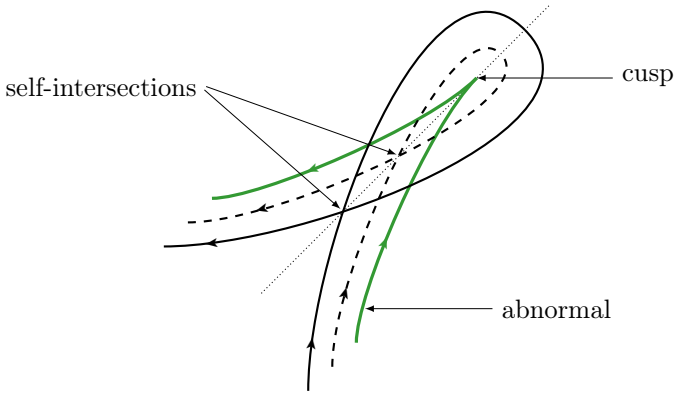

Figure 12: Abnormal with cusp singularity as limit case of self-intersecting normal extremals.

References

[1] D. Bao, S.-S. Chern & Z. Shen, *An Introduction to Riemann-Finsler Geometry*, vol 200 of Graduate Texts in Mathematics, Springer-Verlag New York, 2000, 435 pages.

[2] D. Bao, C. Robles & Z. Shen, *Zermelo navigation on Riemannian manifolds*, J. Differential Geom., **66** (2004), no. 3, pp. 377–435.

[3] M. Berger, *La géométrie métrique des variétés riemanniennes (variations sur la formule* $a^2 = b^2 + c^2 - 2bc\cos\alpha$*)*, dans Élie Cartan et les mathématiques d'aujourd'hui - Lyon, 25-29 juin 1984, Astérisque, no. S131 (1985), pp. 9-66.

[4] B. Bonnard & I. Kupka, *Théorie des singularités de l'application entrée/sortie et optimalité des trajectoires singulières dans le problème du temps minimal*, Forum Math., **5** (1993), no. 2, pp. 111–159.

[5] B. Bonnard, O. Cots, B. Wembe, *A Zermelo navigation problem with a vortex singularity*, (2019) ⟨hal-02296046v2⟩.

[6] A. E. Bryson & Y.-C. Ho, *Applied optimal control*, Hemisphere Publishing, New-York, 1975.

[7] C. Carathéodory, *Calculus of Variations and Partial Differential Equations of the First Order, Part 1, Part 2*, Holden-Day, San Francisco, California, 1965–1967; Reprint: 2nd AMS printing, AMS Chelsea Publishing, Providence, RI, USA, 2001, 412 pages.

[8] R. Hama, J. Kasemsuwan and S. V. Sabau, *The cut locus of a Randers rotational 2-sphere of revolution*, Publ. Math. Debrecen, **93** (2018), no 3-4, pp. 387–412.

[9] L. S. Pontryagin, V. G. Boltyanskiĭ, R. V. Gamkrelidze & E. F. Mishchenko, *The Mathematical Theory of Optimal Processes*, Translated from the Russian by K. N. Trirogoff, edited by L. W. Neustadt, Interscience Publishers John Wiley & Sons, Inc., New York-London, 1962.

[10] K. Shiohama, T. Shioya, and M. Tanaka, *The geometry of total curvature on complete open surfaces,*, Cambridge Tracts in Math., **159** (Cambridge University Press, 2003), 284 pages.

[11] E. Zermelo, *Über das Navigations problem bei ruhender oder veränderlicher wind-verteilung*, Z. Angew. Math. Mech., **11** (1931), no. 2, pp. 114–124.